Analysis of Forces on Ferromagnetic Components Used in Magnetic Fusion Reactors

H. Attaya, G.L. Kulcinski and W.G. Wolfer

September 1983

UWFDM-540

Presented at the Third Topical Meeting on Fusion Reactor Materials, Albuquerque, NM, 19-23 September 1983] [J. Nucl. Matls. **122&123** (1984) 961.

FUSION TECHNOLOGY INSTITUTE

UNIVERSITY OF WISCONSIN

MADISON WISCONSIN

Analysis of Forces on Ferromagnetic Components Used in Magnetic Fusion Reactors

H. Attaya, G.L. Kulcinski and W.G. Wolfer

Fusion Technology Institute
University of Wisconsin
1500 Engineering Drive
Madison, WI 53706

http://fti.neep.wisc.edu

September 1983

UWFDM-540

Presented at the Third Topical Meeting on Fusion Reactor Materials, Albuquerque, NM, 19-23 September 1983 [J. Nucl. Matls. **122&123** (1984) 961].

ANALYSIS OF FORCES ON FERROMAGNETIC COMPONENTS USED IN MAGNETIC FUSION REACTORS

H. ATTAYA, G.L. KULCINSKI, and W.G. WOLFER

Fusion Engineering Program, Nuclear Engineering Department, University of Wisconsin, Madison, WI 53706

The magnetic forces on the coolant pipe of the MARS mirror reactor are calculated and analyzed. The magnitude of these forces is shown to be smaller than those associated with the coolant pressure, but they are not uniform. Such nonuniformity could lead to pipe deformations. It is also shown that the magnetic forces on an equivalent beam with the same material volume provide a reasonable estimate for the total forces on the pipe.

1. INTRODUCTION

In magnetic fusion reactors the use of ferromagnetic steels in the blanket and the first wall has been suggested primarily because of their excellent swelling resistance as compared to austenitic alloys.[1] The presence of such materials in magnetic fusion reactors would have two effects on the design of the device. The first effect is due to the induced magnetic field from these materials which might modify the carefully tailored field profile. The second effect, which is the subject of this paper and a continuation of previous work,[2] is the forces that these magnetic materials will be subjected to and which will require careful design consideration to properly support structural components.

A typical blanket of a fusion reactor consists of a complicated assembly of pipes, beams, supports, etc. To evaluate in detail the magnetization $\overline{M}$ in such complicated structures and consequently calculate the induced field or the magnetic loading would require unprecedented computer resources. Accordingly, one approach has been to homogenize the magnetic material, hereafter referred to simply as iron, within the blanket such that the magnetization density in the homogenized blanket equals the magnetization density of the iron multiplied by the volume fraction of the iron in the blanket. This method has been used primarily to evaluate the induced magnetic field in regions far from the homogenized blanket, e.g. in the plasma region. In other calculations[2] of the magnetic loading, an actual geometry of a pipe has been replaced by a simpler one such as a beam with solid square cross sections.

In this paper we analyze the magnetic forces on an actual pipe and compare it with the forces on the equivalent beam.

2. MAGNETIC FORCES ON A PIPE

The formulae that are used to calculate the magnetic forces are those given by Brown,[3] and are stated below.

The *total* force, $\overline{F}_t$, and the total moment, L_t, on a magnetized body are given by

$$\overline{F}_t = \int_V \overline{M}\cdot\nabla\overline{H}_o \, d\tau \ , \qquad (1)$$

and

$$L_t = \int_V \overline{M}\times\overline{H}_o \, d\tau \ . \qquad (2)$$

However, the magnetic forces on a *part* of the body of volume dV is given by

$$\overline{F}_{dV} = \int_{dV} \overline{M}\cdot\nabla\overline{H} \, d\tau + 2\pi \int \overline{n}\, M_n^2 \, ds \qquad (3)$$

and the magnetic moment on the part dV is

$$\Gamma_{dV} = \int_{dV} \overline{M} \times \overline{H} \, d\tau \, . \qquad (4)$$

Here, $\overline{M}$ is the magnetization density, $\overline{H}_0$ is the magnetic field intensity due to sources outside V, $\overline{H}$ is the total magnetic field intensity in $d\tau$, M_n is the normal component of the magnetization at the surfaces enclosing dV, and $\overline{n}$ is the outward normal to the surface element ds. Gaussian units are employed in these equations.

The above formulae have been incorporated in the computer program GFUN3D.[4]

The section of the pipe that was examined is the shaded part in Fig. 1, and it is 1 m long, 0.43 m in outer diameter, and 0.05 m thick. It extends parallel to the vertical y-axis of the coordinate system indicated in Fig. 1. This figure gives a cross-sectional view along the axis of the MARS central cell,[5] and the pipe in question is close to one of the inlet cooling pipes adjacent to a central cell magnet. The force distribution on this section of the pipe is given at various vertical locations and along the directions of a cylindrical coordinate system whose axis coincides with the axis of the pipe. Due to mirror symmetry with respect to the y-z plane, the force components displayed in Fig. 2 are shown only for one side of the pipe, i.e. for polar angles θ from 0° to 180°. All force components exhibit a strong variation with the polar angle. For example, the radial force (solid curves in Fig. 2) changes from positive to negative values in contrast to the positive radial pressure exerted by the coolant. Although the average radial magnetostatic force per unit area is quite small compared to the coolant pressure, its nonuniform distribution may lead to ovality when the pipe can deform significantly by thermal creep.

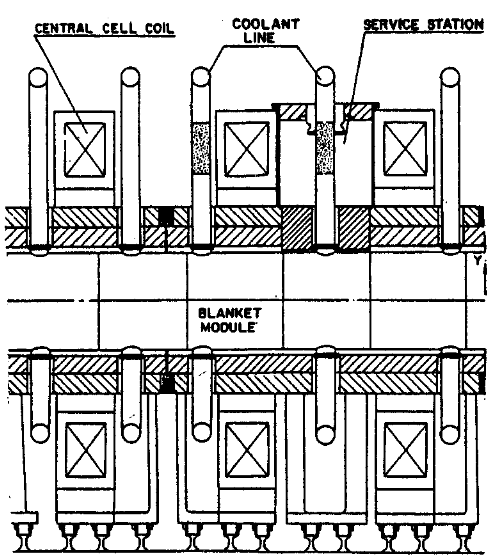

FIGURE 1
Cross section for MARS blanket.

Furthermore, the sum of the radial and circumferential force distribution results in a net force on the pipe which lies in the y-z plane of the central cell coordinate system.

It is also interesting to note that the force component parallel to the pipe axis (chaindotted curves in Fig. 2) varies along the circumference. This leads also to a bending moment distribution along the pipe which must be added to the bending moment caused by the net force distribution perpendicular to the pipe axis.

The body moment distribution as calculated with Eq. (4) turns out to be $< 10^{-7}$ Nm and may be neglected. This negligible body moment is a reflection of the fact that the field at the volume element under consideration is greater than 3 T and beyond the value for saturation. Hence magnetization and local field directions are parallel.

A crude estimate of potential stresses that the above magnetostatic forces could produce was obtained by considering the pipe to be clamped at one end and the total magnetostatic force applied at the free end. In this case, a maximum stress of about 43 MPa is developed.

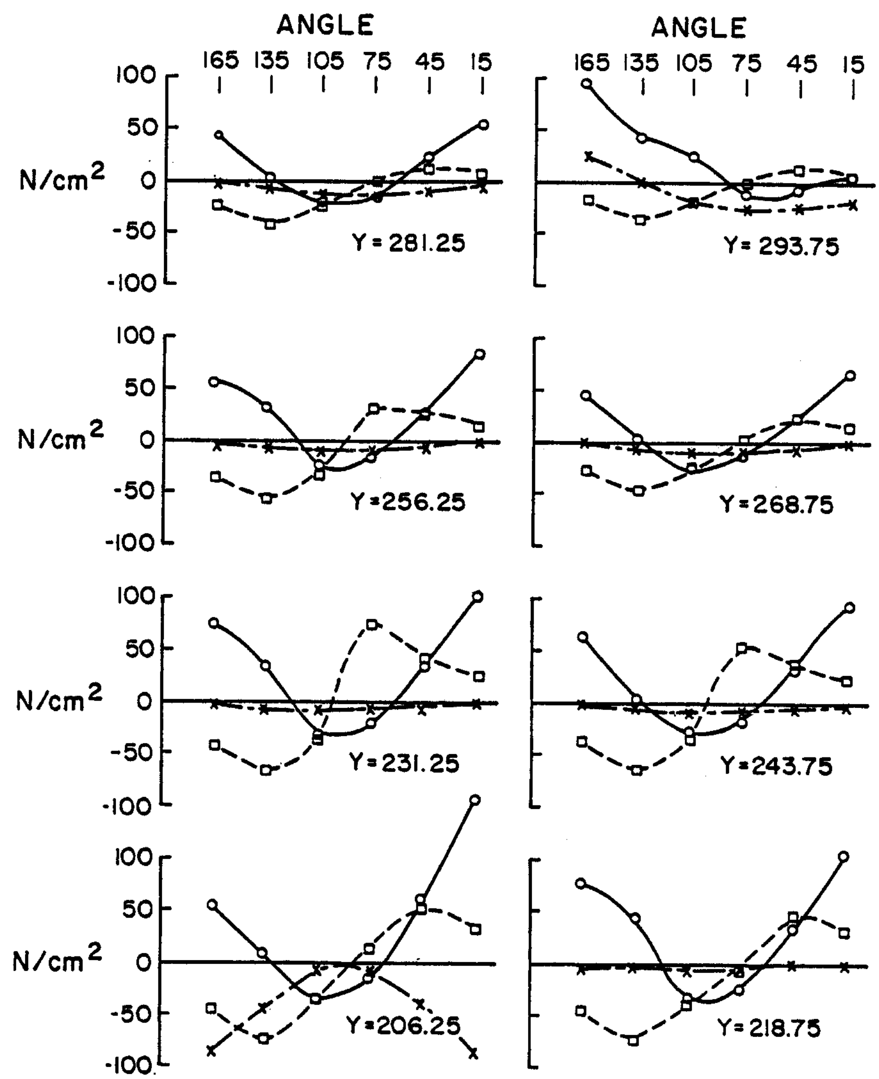

FIGURE 2
Magnetostatic force components per unit area on the pipe adjacent to the magnet as a function of the vertical position (y) and the circumferential angle. Solid line (-o-) is the radial component, dashed line (-□-) the circumferential, and the chain dotted line (-x-) is the vertical component.

When components are located in positions where a high degree of magnetic field symmetry exist, the magnetostatic forces can be reduced dramatically. Consider, for example, the pipe located precisely midway between two adjacent central cell magnets. The radial and circumferential force components exhibit mirror symmetry with respect to the x-y and the y-z planes, and a total force on the pipe exists only in the vertical y-direction and is equal to -1.3×10^5 N. However, this symmetry location is an unstable one with regard to small displacements or deflections of the pipe. This was indeed confirmed by actual calculations showing clearly that a net force develops in the direction that tends to increase the displacement. Therefore, supports should even be provided for those components that experience no net force because of symmetry considerations.

3. FORCES ON EQUIVALENT BEAM

As mentioned before, the magnetic force calculation on an actual pipe is fairly expensive, because a thin wall pipe requires a large amount of iron elements to be simulated in GFUN. Even if one makes use of the symmetry of the problem under consideration, one cannot exceed the maximum aspect ratio of the iron elements that is allowed in GFUN. Accordingly, other alternatives have been explored to avoid expensive calculations and to provide the designer with a reasonably accurate estimate of the magnetic forces on such pipes. The geometry of a simple beam requires substantially less elements for the force evaluation. An equivalent beam of square cross-section and equal iron volume is placed with its axis to coincide with the axis of the actual pipe. The force distribution along the vertical extension is computed on one-half of the beam or pipe, i.e. on the part on one side of the y-z symmetry plane. The force components are now given for the cartesian frame indicated in Fig. 1, and plotted for comparison in Fig. 3 for the case that the pipe or beam are adjacent to one central cell magnet. The comparison between the force components on the pipe and on the equivalent beam shows that the forces in the y and z directions are reasonably close, but the forces in the x direction show considerable differences for the following reasons.

The force on a volume element [Eq. (3)] increases when it is exposed to a higher field gradient $\nabla\vec{H}$. It also increases when the normal component of the magnetization, M_n, in-

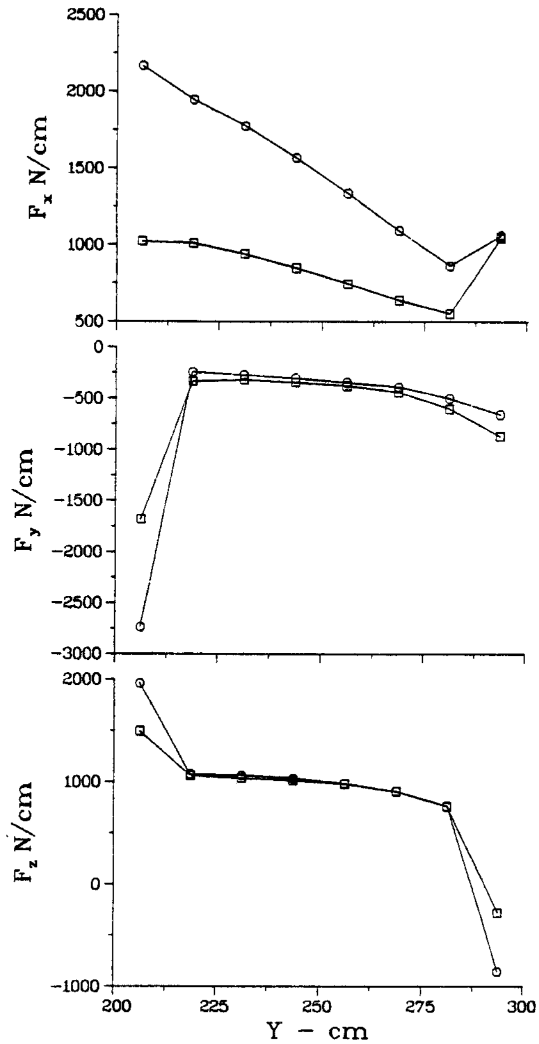

FIGURE 3
Comparison between the magnetic forces on half of the pipe (o), and the magnetic forces on half of the equivalent beam (□) placed adjacent to the magnet.

creases at surface elements oriented in the direction of the force component to be considered. Thus, there are two effects which contribute to the difference. First, the iron material in the case of the pipe is, on average, farther from the symmetry plane and hence exposed to a higher field gradient than in the case of the equivalent beam. This explains the major difference between the F_x force components. The second effect arises from the difference in the demagnetization factors for bodies of different shape. For the beam case, M_n nearly vanishes on the flat surfaces perpendicular to the x-direction. Hence the surface integral in Eq. (3) makes almost no contribution to the force F_x. In contrast, M_n on the pipe surface is substantial, and hence the surface integral contributes to F_x and makes its value larger than that for the equivalent beam.

If the pipe or the beam is placed midway between two central cell magnets, as is the case for the coolant pipe at the service stations in Fig. 1, the forces F_z along the axis of the machine should vanish. These forces are shown in Fig. 4. The small magnitude of this component F_z at this symmetrical position must be considered as the absolute error in our calculations. The behavior of F_x and F_y is similar to that shown in Fig. 3.

It should be noted that the total force in the x-direction is the sum of the forces on the two halves of the cross section as divided by the symmetry plane. When located perfectly symmetric, it of course vanishes. However, when slightly displaced from the symmetry position, the total horizontal force F_x is no longer zero. Therefore, for stability and buckling investigations, differences in the forces for the actual pipe and an equivalent beam can become of particular significance. When only the global forces on a pipe are of interest, the pipe may be simulated by an equivalent solid beam.

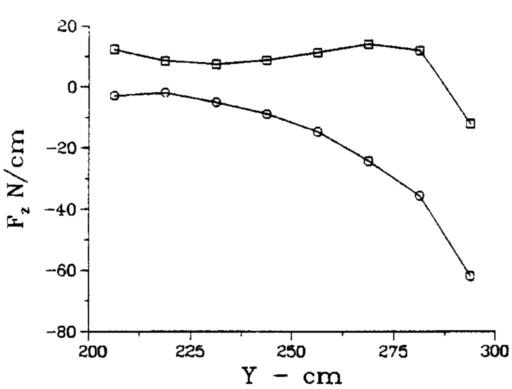

FIGURE 4
Comparison between the axial component of the magnetic forces on half of the pipe (o) and half of the equivalent beam (▫) placed midway between two magnets.

4. CONCLUSIONS

The magnetic loading on a part of the coolant pipe for the MARS reactor was analyzed. It is shown that the magnitude of the magnetic force is small compared to the coolant pressure, and the distribution of the magnetic force is not uniform. The nonuniformity of these forces may lead to ovality when the pipe is deformed under thermal creep. It is also shown that the magnetic forces on the main coolant pipes are not stable for small lateral displacements. Finally, it is shown that for the purpose of designing the support structure for the pipes, the pipe could be simulated by an equivalent solid beam configuration.

REFERENCES

1. J.J. Sniegowski and W.G. Wolfer, Proc. of Conf. on Ferritic Alloys for Use in Nuclear Energy Technologies, Snowbird, Utah, USA, June 1983, to be published.

2. H. Attaya, K.Y. Yuan, G.L. Kulcinski, and W.G. Wolfer, ibid.

3. W.F. Brown, Magnetoelastic Interactions, (Springer-Verlag, Berlin, 1966).

4. A.G. Armstrong, C.J. Collie, N.J. Diserns, M.J. Newman, J. Simkin, and C.W. Trowbridge, "GFUN3D User Guide," 2nd Ed., RL-76-029, 1979.

5. "Mirror Advanced Reactor Study (MARS) Interim Design Report," UCRL-53333, Lawrence Livermore National Laboratory (1983).